



Statistical analysis of solid-state recycled aluminum alloy 2011 chips by hot extrusion

Original
Article

Bola Wagdy, Ayman A. Abd El-Wahab, Ramadan El-gamasy

Department of Design and Production Engineering, Ain Shams University, Cairo, Egypt

Keywords:

Aluminum chips, design of experiments, hot extrusion, solid-state recycling

Corresponding Author:

Bola Wagdy, Department of Design and Production Engineering, Ain Shams University, Cairo, Egypt, Tel:+20 109 008 9322, Email: bolawagdy8@gmail.com

Abstract

The conventional recycling method of aluminum by remelting the scraps is causing environmental problems, material losses, and depletion of energy resources. This paper aims to present an eco-friendly recycling technique for the aluminum alloy AA2011. The chips obtained from the turning operation were collected, compacted into billets, and hot extruded. Experiments were planned according to the design of experiments (DOE) approach. The recycling process parameters were extrusion temperature and ratio. Regression analysis (RA) and analysis of variance (ANOVA) were conducted, and significant mathematical models were obtained. The adopted equations demonstrated the effect of the extrusion parameters on the ultimate tensile strength and the yield strength of the extruded aluminum. The results showed that the extrusion temperature and the extrusion ratio significantly influenced the tensile and yield strengths of the samples. An Optimization process was carried out to maximize the abovementioned mechanical properties of the extrudates. Metallographic analysis was also performed to study the bonding quality between the chips.

1. INTRODUCTION

Aluminum recycling is a valuable operation that decreases the reduction of the original reserves of this metal. The recycling process has both economic and ecological benefits. According to Gaušad *et al.*, the extraction of aluminum, also called primary production, causes harmful environmental impacts such as the emission of hazardous gases including carbon dioxide CO₂, the generation of solid waste, and the depreciation of the landscape^[1]. Moreover, in terms of energy consumption, the primary production of aluminum is one of the most energy-intensive production processes because it needs (168-200) GJ/ton, which surpasses the production energy of steel by a factor of ten^[2].

The recycling process consists of two major methods: the conventional remelting method (known as secondary production) and the non-remelting recycling method (also called solid-state recycling). For the remelting process, several problems occur listed as follows: (1) generation of toxic and greenhouse gases that pollute the air and increase global warming, (2) chemical reactions that cause up to 25% material (aluminum) losses, and (3) high energy consumption that can reach up to (16-19) GJ/ton^[3]. According to Koch *et al.*, the solid-state recycling method requires about 3.2 GJ/ton with almost no material losses^[4]. Based on these facts, the non-remelting method offers a valuable alternative for recycling aluminum chips. The solid-state recycling process consists of collecting,

cleaning, compacting the chips, and applying severe plastic deformation (SPD) techniques. Also, another method of recycling is to mill the chips into powder and apply powder metallurgy (PM) manufacturing techniques^[5]. In recent years, many studies were conducted on solid-state recycling of non-ferrous metals including aluminum. For example, Kadir *et al.* investigated the microhardness of cold-forged mixtures of AA6061 chips and powders. It was found that the mixture including 78.5% powder of size 25 μm and 21.5% powder of size 100 μm had 25% lower microhardness compared to the original material^[6]. Abd El Aal *et al.* studied the effect of extrusion temperature and extrusion ratio on the mechanical properties and the microstructure of solid-state recycled AA6061 chips. The cold compacted chips were hot extruded at three extrusion ratios (R = 5.2, 7.7, and 12.8) and three extrusion temperatures (T = 350, 425, and 500 °C). The results showed that the hot extrusion technique produced extrudates with densities up to 100%. Optimum tensile strength, percent elongation, and bonding quality between chips were achieved at R = 12.8 and T = 500 °C^[7]. Kuddus *et al.* investigated the physical characteristics of solid-state recycled AA6061 chips reinforced with silicon carbide (SiC). Preheating temperatures were T = 450, 500, and 550 °C, and preheating times were t = 1 and 3 hours. The weight percentages of SiC were wt.% = 5, 10, and 15. Extrusion ratio was constant at R = 5.3. The results showed

that extruded materials at $T = 550\text{ }^{\circ}\text{C}$, $t=1\text{-hour}$, and $\text{SiC wt.\%} = 5$ had a microstructure with the lowest grain size and a density equal to the original material density^[8].

Furthermore, some researchers planned their experiments based on the design of experiments (DOE) methods. For example, Lela *et al.* set up experiments to solid-state recycle AW2011 chips using the Box-Behnken design (BBD) method. Regression analysis (RA) and analysis of variance (ANOVA) developed mathematical models having significant terms that described the effect of depth of cut ($a = 0.5, 1.125, \text{ and } 1.75\text{ mm}$), extrusion temperature ($T = 300, 400, 500\text{ }^{\circ}\text{C}$), and compaction force ($F = 200, 350, \text{ and } 500\text{ kN}$) on yield strength, tensile strength, and percent elongation. Extrusion ratio was constant at $R = 7.1$. The results showed that the optimal process parameters ($a = 1.75\text{ mm}$, $T = 358\text{ }^{\circ}\text{C}$, and $F = 200\text{ kN}$) that maximized the abovementioned mechanical properties led to the presence of cracks in the microstructure^[9]. Also, Ragab *et al.* used the BBD method to generate experimental points for solid-state recycling AA6061 chips. RA and ANOVA generated quadratic models that related surface roughness to significant turning parameters. The machining parameters were cutting speed ($v = 100, 150, \text{ and } 200\text{ m/min}$), feed ($s = 0.012, 0.081, \text{ and } 0.15\text{ mm/rev}$), and depth of cut ($a = 0.1, 0.25, \text{ and } 0.40\text{ mm}$). The cold compacted chips were hot extruded at $350, 425, \text{ and } 500\text{ }^{\circ}\text{C}$. The extrusion ratio was constant at $R = 5.2$. The results showed that the feed was the most significant parameter affecting the surface quality. The optimum machining conditions were $v = 116\text{ m/min}$, $s = 0.11\text{ mm/rev}$, and $a = 0.33\text{ mm}$ when the extrusion temperature was $500\text{ }^{\circ}\text{C}$. The sample produced under these conditions had a surface roughness R_a below the industrially accepted value^[10]. Moreover, Krolo *et al.* studied the effect of direct extrusion temperature ($400, 450, \text{ and } 500\text{ }^{\circ}\text{C}$), ECAP temperature ($20, 160, \text{ and } 300\text{ }^{\circ}\text{C}$), and ECAP pass number ($1, 3, \text{ and } 4$) on microhardness and electrical conductivity of solid-state recycled AW6082 chips. The extrusion ratio was constant at $R = 7.1$. The test runs were planned according to BBD. Also, an adaptive neuro-fuzzy interference system (ANFIS) and regression analysis (RA) were conducted. The results implied that the increase in the extrusion temperature increased the microhardness and decreased the electrical conductivity, while the ECAP temperature had a contrary behavior^[11]. Sabbar *et al.* applied the central composite design (CCD) for solid-state recycling of AA7075 chips reinforced by zirconium dioxide (ZrO_2) nanoparticles by direct extrusion and ECAP, then followed by heat treatment. The extrusion ratio and temperature were 5.4 and $300\text{ }^{\circ}\text{C}$, respectively. The factorial design parameters were ZrO_2 volume fraction ($\text{VF}\% = 1, 3, \text{ and } 5$), heat treatment temperature ($T = 450, 500, 550\text{ }^{\circ}\text{C}$), and heat treatment time ($t = 1, 2, \text{ and } 3\text{ hours}$). The results showed that the optimum density, hardness, and tensile strength were obtained at $\text{VF}\% = 1$, $T = 550\text{ }^{\circ}\text{C}$, and $t = 1.58\text{ hours}$ ^[12].

After reviewing the literature, only the work of Lela *et al.* was found investigating the aluminum alloy 2011 despite its exceptional machinability. So, the main aim of

this paper is to develop mathematical models that describe the effect of extrusion temperature and extrusion ratio on the mechanical properties of solid-state recycled AA2011 chips.

2. Methodology

2.1. Machining and Cold Compaction

The chips were produced by turning an aluminum alloy 2011 shaft $\phi 50 \times 1500\text{ mm}$ on a lathe machine using high-speed steel (HSS) cutting tool. The aluminum bar was in the T6 condition. The chemical composition of the aluminum alloy was measured using a SPECTROMAXx Spectrometer (arc/spark OES). The chemical composition is presented in Table 1. Dry machining was applied because cleaning the chips from the coolant was not available. According to Shamsudin *et al.*, The cutting fluid would contaminate the chips which would result in changing the microstructure of the extrudates, impairing the bonding quality between the chips, thus reducing the mechanical properties of the extruded solid^[13]. The maximum available cutting speed on the lathe was about 45 m/min . This speed, with any positive rake angle tool, caused the formation of long continuous chips that promoted the formation of a build-up edge (BUE). BUE would change the depth of cut due to the cold pressure welding of the chips on the tool face. Therefore, the cutting conditions and the tool angles were selected to ensure the formation of discontinuous chips (segments) to minimize or eliminate BUE formation. The cutting conditions and the tool angles are shown in Table 2.

Table 1: Chemical composition of AA2011

Si%	0.05	Bi%	0.50
Fe%	0.38	Pb%	0.34
Cu%	4.55	Other%	0.14
Zn%	0.04	Al%	94.00

Table 2: The cutting conditions and the tool angles

Cutting Conditions	Speed (v)	5 m/min
	Feed (s)	0.8 mm/rev
	Depth of Cut (a)	1 mm
HSS Tool Angles	Rake (γ)	-5°
	Clearance (α)	9°

The obtained chips from the turning operation are shown in Figure 1.



Fig. 1: Aluminum alloy 2011 chips

The geometry of the chips is shown in Table 3.

Table 3: The geometry of the chips in mm

Length (lavg)	13.05
Width (wavg)	1.84
Thickness (tavg)	1.75

The cold compaction of the chips into billets was done using a 100-ton hydraulic press and a compacting rig of 39 mm inner diameter. Figure 2 shows the compacting rig and the hydraulic press.



Fig. 2: The compacting rig and the hydraulic press

In agreement with the work of Misiolek *et al.*, a multi-layer compaction technique was applied to prepare the chip-based billets. Each billet had a constant mass of 125 g and required four steps of compaction until the compacted billet had an average height of 47 mm. Figure 3 shows an example of a compacted chip-based billet.

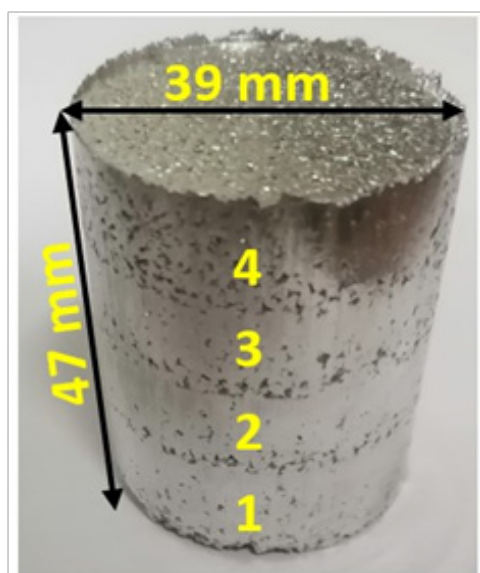


Fig. 3: A compacted chip-based billet

2.2. Design of Experiments (DOE)

Full factorial design (FFD) was applied to set up the experiments. Two parameters of interest were chosen, namely, the extrusion temperature (A) and the extrusion ratio (B). Each factor had 3 levels: the extrusion temperatures were 350, 425, and 500 °C, while the extrusion ratios were 6, 8, and 10. The number of experiments (N) is given by the equation $N = n^k$, where n and k are the number of levels and the number of parameters, respectively. Design-Expert software package was used to generate the nine experimental runs shown in Table 4.

Table 4: FFD experimental runs

Run	Extrusion Temperature, (A) in °C	Extrusion Ratio, (B)
1	350	10
2	350	8
3	500	8
4	500	6
5	425	8
6	425	6
7	350	6
8	425	10
9	500	10

2.3. Hot Extrusion

The hot extrusion process was performed utilizing the same rig and the same hydraulic press used for the compaction of the chips. In order to produce the samples, three flat-faced dies were manufactured, according to the selected extrusion ratios. Each die had a square hole with a fillet (r). The square hole profiles of the dies are shown in Figure 4. The punch speed was 8 mm/s. The die, the container, and each billet were heated in the furnace at the corresponding extrusion temperature. The furnace temperature was kept constant, after reaching the desired temperature, for 1-hour to ensure temperature homogeneity.

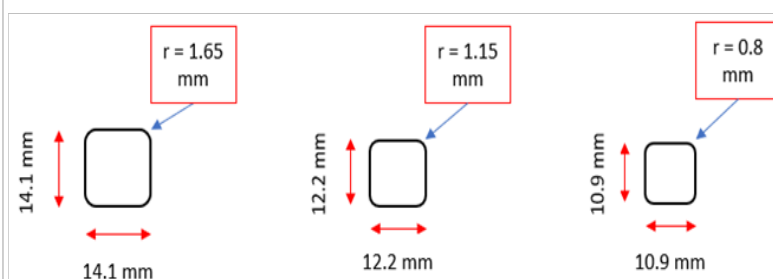


Fig. 4: Square hole profiles of the dies

3. Results and Discussion

3.1. Extruded Samples

All the extrusion processes were successful and solid square bars were obtained. Before physical and mechanical testing, the nine extruded samples were visually inspected. All the extrudates had a high-quality surface finish.

Due to insufficient shear deformation at the start of the extrusion process, the beginnings of all the samples had either a flower profile or a pills profile, where chips could be seen clearly. These profiles were independent of both the extrusion temperature and ratio. Figure 5 shows an example of two extruded samples having this phenomenon.

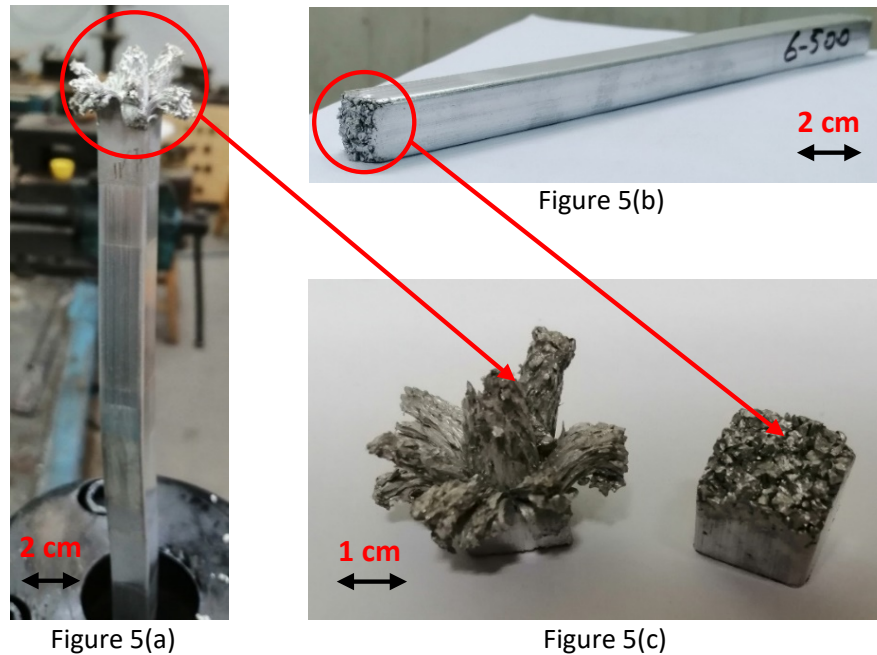


Fig. 5 : (a) A sample with a flower profile, (b) a sample with a pills profile, and (c) flower and pills profiles

3.2. Density

The density test was conducted based on the principle of Archimedes. An Aczet CY 224C device was used to calculate the densities of the original material and the extruded samples. The density of the ingot material was $2,800 \text{ kg/m}^3$, while the densities of the extrudates varied between $2,800$ and $2,810 \text{ kg/m}^3$. Higher densities could be due to the presence of aluminum oxide Al_2O_3 inside the samples. Al_2O_3 has a higher density that can reach up to $3,980 \text{ kg/m}^3$.

samples, a universal testing machine (Lloyd LR 300K) was used. According to ASTM E8, tensile test specimens were prepared on a lathe having a gauge diameter, a gauge length, and a reduced length of 4, 16, and 20 mm, respectively. The test speed was 5 mm/min. Three specimens of each extruded sample were manufactured, and mean values and standard deviations were calculated. Most of the specimens showed a shear fracture which was expected from a ductile material. However, some specimens showed a brittle fracture. These specimens were from the closest section to the beginning of the extrusion process where insufficient shear deformation occurred to ensure appropriate bonding between the chips. Figure 6 shows brittle and ductile fractures of two specimens of sample 9.

3.3. Tensile Testing

In order to determine the mechanical properties of the



Fig. 6: Sample 9: specimen with brittle fracture (left) and specimen with ductile fracture (right)

The yield strength was calculated by applying the 0.2% offset method. The engineering stress-strain curves of the three specimens of sample 9

and the original material specimen are shown in Figure 7. The brittleness behavior is also shown.

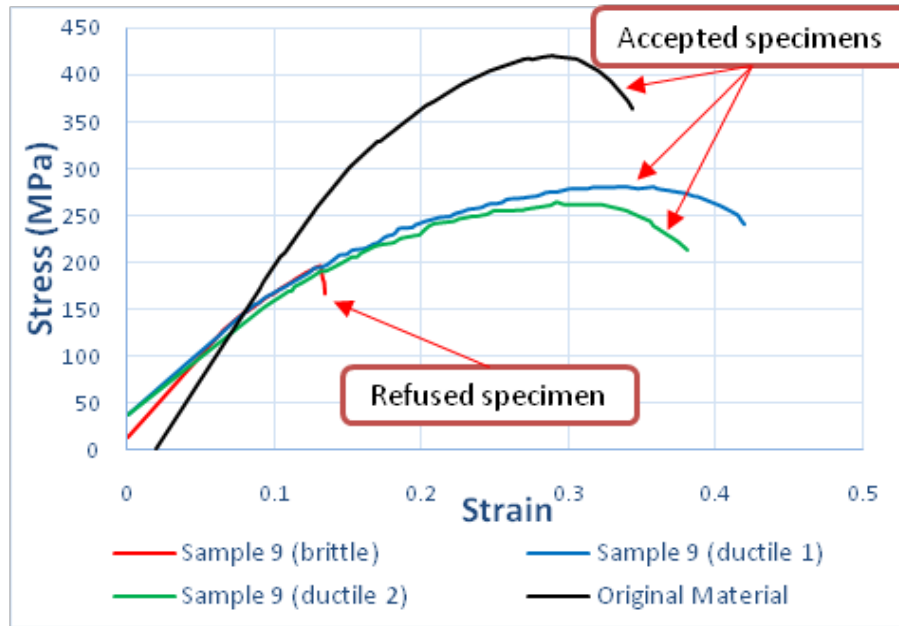


Fig. 7: Engineering stress-strain curves of sample 9 and original material

The ultimate tensile strength (Rm), the yield strength (Rp0.2), and the percent elongation (PE) of the nine samples and the standard material are shown in Table 5. Standard deviation was not calculated for any sample that had a brittle specimen showing abnormally

low (non-representative) properties. As a result, these specimens were rejected, and the average values of the properties were used instead. Therefore, the rejection percentage was about 13.3% (4 refused specimens from 30 tensile test specimens).

Table 5: Mechanical properties of the samples and the original material

Sample	A (°C)	B	Rm (MPa)	Rp0.2 (MPa)	PE (%)
1	350	10	207.0 ± 5.0	141.0 ± 9.9	21.8 ± 5.0
2	350	8	202.7 ± 5.9	135.7 ± 1.2	23.9 ± 2.1
3	500	8	234.5	150.5	21.1
4	500	6	265.5	159.0	21.5
5	425	8	211.0 ± 8.6	135.7 ± 1.2	21.0 ± 0.9
6	425	6	194.0	141.0	26.5
7	350	6	183.7 ± 8.1	137.7 ± 10.6	21.6 ± 4.9
8	425	10	221.0 ± 17.1	151.0 ± 4.5	23.2 ± 3.9
9	500	10	272.0	160.0	25.9
Standard			425.0 ± 7.8	224.3 ± 9.8	18.2 ± 3.4

The obtained mechanical properties of the samples were inserted into the Design-Expert software package. Regression analysis (RA) and analysis of variance (ANOVA) were performed and mathematical

models for Rm and Rp0.2 were developed. According to regression and variance analysis, PE could not be represented by any mathematical equation having significant terms.

3.4. Regression and Variance Analysis for Ultimate Tensile Strength

According to RA and ANOVA, a reduced quadratic mathematical model was suggested for R_m . The results showed that only the extrusion temperature (A) was a significant model term with a P -value of 0.0032. R-squared was obtained as 0.8742. The Predicted R-squared of 0.6249 and the Adjusted R-squared of 0.7987 were in reasonable agreement, as the difference is less than the required value

of 0.2. So, the developed model was not overfitted. Adeq (adequate) Precision, which is the measurement of signal-to-noise ratio, was obtained as 8.559 while the minimum desirable ratio is 4. The mathematical equation of R_m in terms of the actual factors is represented by equation (2).

$$R_m = 609.02222 - 2.45911A + 4.73333B + 0.003360A^2(2)$$

Figure 8 shows the graphical representation of the R_m equation.

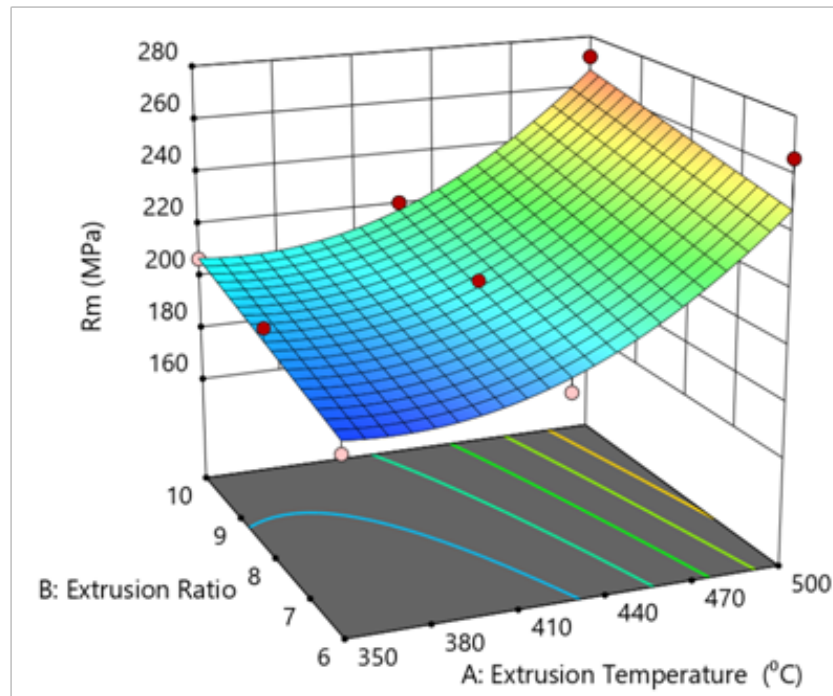


Fig. 8: Effect of the extrusion temperature and ratio on the ultimate tensile strength of the extrudates

3.5. Regression and Variance Analysis for Yield Strength

According to RA and ANOVA, a reduced quadratic mathematical model was suggested for $R_{p0.2}$. The results showed that the extrusion temperature (A) and the square of the extrusion ratio (B^2) were significant model terms with p -values of 0.0016 and 0.0256, respectively. R-squared was 0.9517. The Predicted R-squared and the

Adjusted R-squared were 0.7555 and 0.9034, respectively. Adeq Precision was obtained as 12.76. The mathematical equation of $R_{p0.2}$ in terms of the actual factors is represented by equation (3).

$$R_{p0.2} = 330.69630 - 0.529852A - 27.67500B + 0.000767A^2 + 1.80417B^2(3)$$

Figure 9 shows the graphical representation of the $R_{p0.2}$ equation.

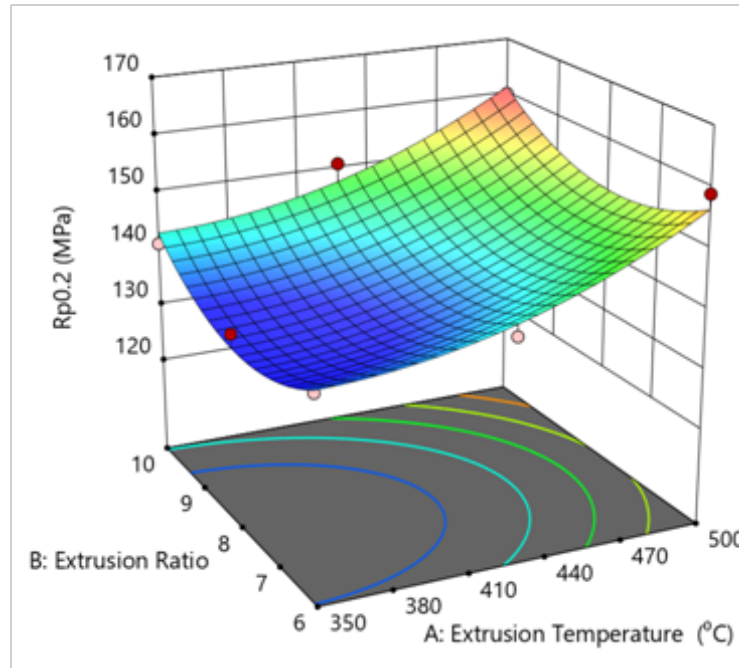


Fig. 9: Effect of the extrusion temperature and ratio on the yield strength of the extrudates

3.6. Percent Elongation

RA and ANOVA showed that PE could not be modeled with any significant mathematical model. The analysis implied that the overall mean of 22.94% with a standard deviation of 1.96 might be the better predictor of the percent elongation of all the samples.

3.7. Optimization

For the optimization, the goal was to maximize both

Rm and Rp0.2, while the average PE of 22.94% was used. The solution that had the highest desirability factor, which varies between 0 (lowest) and 1 (highest), was chosen. Sample 9 (A = 500 °C and B = 10) satisfied such condition having a desirability factor of 0.97. The maximum obtained Rm and Rp0.2 were 266.8 MPa and 161.3 MPa, respectively.

Figure 10 shows the graphical representation of the optimization process.

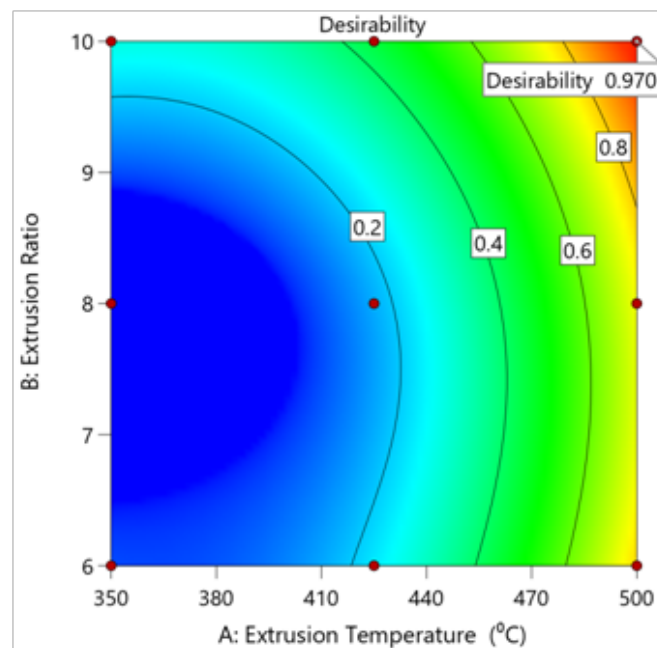


Fig. 10: The desirability factors of the optimization process

3.8. Metallographic Analysis

In order to determine the bonding quality between the chips, a microstructure analysis was conducted. The process included cutting, grinding, polishing, and etching metallographic specimens. Then, the specimens were observed by an optical microscope with 10× magnification. The resulting metallographic photos showed cracks at

specific sections of all the extrudates. The samples extruded at higher extrusion temperatures and ratios had smaller propagation of the cracks. Higher temperature caused higher friction between the chips, while the increase of the extrusion ratio increased the shear deformation applied to the chips. Consequently, better bonding quality between the chips and higher mechanical properties were obtained. Figure 11 shows micrographs of selected samples.

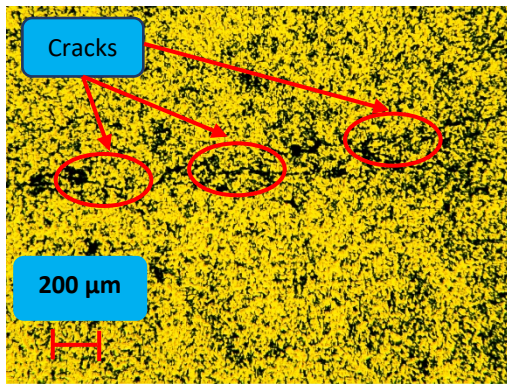


Figure 11(a)

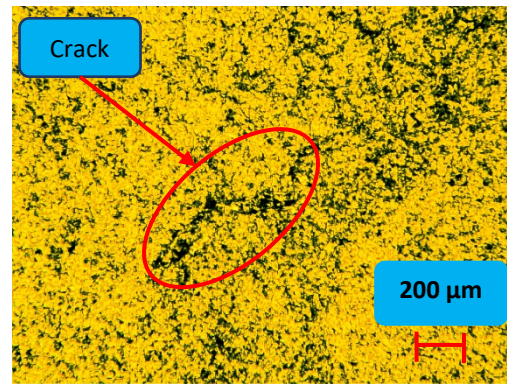


Figure 11(b)

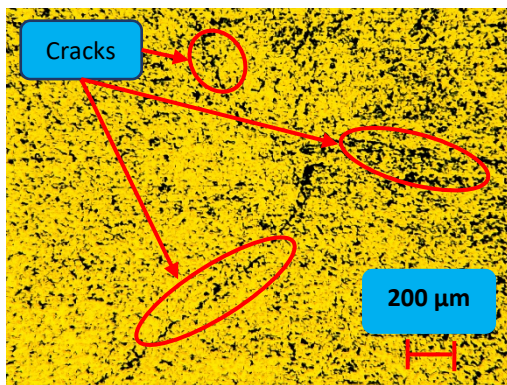


Figure 11(c)

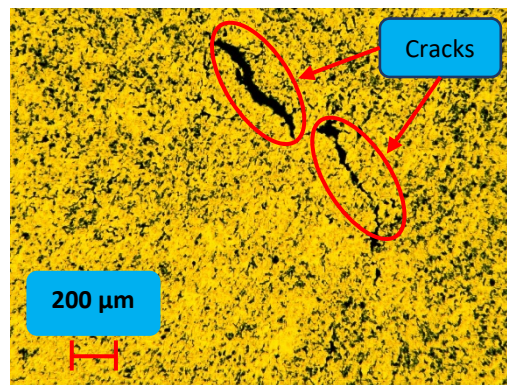


Figure 11(d)

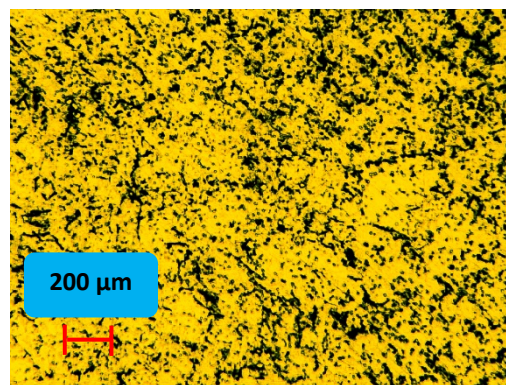


Figure 11(e)

Fig. 11: Micrographs of (a) sample 7, (b) sample 4, (c) sample 1, (d) sample 9, and (e) original material

4. Conclusion

The solid-state recycling of AA2011 chips by hot extrusion was a successful process that produced bars that had comparable physical and mechanical properties to the original material.

1. The extrudates had densities equal to or higher than the reference material, which could be caused by the presence of aluminum oxides Al_2O_3 inside these samples.

2. Through the performed experiments, the ultimate tensile strength (Rm) was influenced only by the extrusion temperature. A maximum Rm of 272 MPa (64% of the reference Rm) was obtained at an extrusion temperature and a ratio of 500 °C and 10, respectively.

3. The yield strength (Rp0.2) was experimentally influenced by both the extrusion temperature and the extrusion ratio. A maximum Rp0.2 of 160MPa (71.3% of the reference Rp0.2) was obtained at an extrusion temperature and a ratio of 500 °C and 10, respectively.

4. The percent elongation (PE) was not influenced by the extrusion temperature and the extrusion ratio. The behavior of PE was complex to be described by any mathematical model. The average PE of 22.94% was adopted instead. The ductility of the extrudates was 26% higher than the ductility of the original material.

5. According to the optimization process, the recycling process parameters that maximized the mechanical properties of the extrudates were found. Maximum Rm and Rp0.2 of 266.8 MPa and 161.3 MPa, respectively, were obtained at an extrusion temperature and a ratio of 500 °C and 10, respectively.

6. The metallographic analysis showed that all the extrudates had cracks. Consequently, the recycled product is industrially unusable. In order to increase the mechanical properties of the solid-state recycled samples and obtain microstructures without cracks, the hot extrusion process should be followed by severe plastic deformation (SPD) processes. During SPD processes, large shear deformation occurs that breaks down the oxide layers formed on chips, thus enabling better bonding between the chips. SPD processes include hot rolling and equal channel angular pressing (ECAP). Also, heat treatment techniques could be applied as the used AA2011 is heat treatable.

5. Acknowledgment

The authors thank Dr. Hala Hassan for facilitating the experimental work inside the metal forming workshop and Mr. Mohamed Zaky for his

contribution while preparing the metallographic specimens.

6. References

- [1] Gaustad, G., Olivetti, E., and Kirchain, R. (2012). Improving aluminum recycling: A survey of sorting and impurity removal technologies. *Resources, Conservation and Recycling*, 58, 79-87. <https://doi.org/10.1016/j.resconrec.2011.10.010>
- [2] Worrell, E., Price, L., Martin, N., Farla, J., and Schaeffer, R. (1997). Energy intensity in the iron and steel industry: A comparison of physical and economic indicators. *Energy Policy*, 25(7-9), 727-744. [https://doi.org/10.1016/s0301-4215\(97\)00064-5](https://doi.org/10.1016/s0301-4215(97)00064-5)
- [3] Gronoštajski, J., Marciniak, H., and Matuszak, A. (2000). New methods of aluminium and aluminium-alloy chips recycling. *Journal of Materials Processing Technology*, 106(1-3), 34-39. [https://doi.org/10.1016/s0924-0136\(00\)00634-8](https://doi.org/10.1016/s0924-0136(00)00634-8)
- [4] Koch, A., Henkel, T., and Walther, F. (2021). Mechanism-oriented characterization of the anisotropy of extruded profiles based on solid-state recycled EN AW-6060 aluminum chips. *Engineering Failure Analysis*, 121. <https://doi.org/10.1016/j.engfailanal.2020.105099>
- [5] Sherafat, Z., Paydar, M. H., and Ebrahimi, R. (2009). Fabrication of Al7075/Al, two phase material, by recycling Al7075 alloy chips using powder metallurgy route. *Journal of Alloys and Compounds*, 487(1-2), 395-399. <https://doi.org/10.1016/j.jallcom.2009.07.146>
- [6] Kadir, M. I., Mustapa, M. S., Mahdi, A. S., Kuddus, S., and Samsi, M. A. (2017). Evaluation of hardness strength and microstructures of recycled chip and powder AA6061 fabricated by cold compaction method. *IOP Conference Series: Materials Science and Engineering*, 165. <https://doi.org/10.1088/1757-899x/165/1/012012>
- [7] Abd El Aal, M. I., Taha, M. A., Selmy, A. I., El-Gohry, A. M., and Kim, H. S. (2018). Solid state recycling of aluminium AA6061 alloy chips by hot extrusion. *Materials Research Express*, 6(3). <https://doi.org/10.1088/2053-1591/aaf6e7>
- [8] Kuddus, S., Mustapa, M. S., Ibrahim, M. R., Shamsudin, S., Lajis, M. A., and Wagiman, A. (2019). Physical Characteristics of Solid State Recycled Aluminum Chip AA6061 Reinforced with Silicon Carbide (SiC) by using Hot Extrusion Technique. *Journal of Physics: Conference Series*, 1150. <https://doi.org/10.1088/1742-6596/1150/1/012004>
- [9] Lela, B., Krolo, J., and Jozić, S. (2016). Mathematical modeling of solid-state recycling of aluminum chips. *The International Journal of Advanced Manufacturing Technology*, 87(1-4), 1125-1133. <https://doi.org/10.1007/s00170-016-8569-5>
- [10] Ragab, A. E., Taha, M. A., Abbas, A. T., Al Bahkali, E. A., El-Danaf, E. A., and Aly, M. F. (2017). Effect of extrusion temperature on the surface roughness of solid state recycled aluminum alloy 6061 chips during turning operation. *Advances in Mechanical Engineering*, 9(10). <https://doi.org/10.1177/1687814017734152>
- [11] Krolo, J., Lela, B., Švagelj, Z., and Jozić, S. (2018). Adaptive neuro-fuzzy and regression models for predicting microhardness and electrical conductivity of solid-state recycled EN AW 6082. *The International Journal of Advanced Manufacturing Technology*, 100(9-12), 2981-2993. <https://doi.org/10.1007/s00170-018-2893-x>
- [12] Sabbar, H. M., Leman, Z., Shamsudin, S., Tahir, S. M., Jaafar, C. N., Ariff, A. H., Zahari, N. I., and Rady, M. H. (2021). The Effect of Solid-State Processes and Heat Treatment on the Properties of AA7075 Aluminum Waste Recycling Nanocomposite. *Materials*, 14(21), 6667. <https://doi.org/10.3390/ma14216667>
- [13] Shamsudin, S., Zhong, Z. W., Rahim, S. N., and Lajis, M. A. (2016). The influence of temperature and preheating time in extrudate quality of solid-state recycled aluminum. *The International Journal of Advanced Manufacturing Technology*, 90(9-12), 2631-2643. <https://doi.org/10.1007/s00170-016-9521-4>